

Study of Kapton Insulated Superconducting Coils Manufactured for the LHC Inner Triplet Model Magnets at Fermilab

N. Andreev, T. Arkan, R. Bossert, J. Brandt, D.R. Chichili, J. Kerby,
A. Nobrega, I. Novitski, J. Ozelis, S. Yadav, A.V. Zlobin

Technical Division, Fermilab, Batavia, Il. 60510 (USA)

Abstract—Fermilab has constructed a number of 2m model quadrupoles as part of an ongoing program to develop and optimize the design of quadrupoles for the LHC Interaction Region inner triplets. The quadrupole design is based upon a two layer shell type coil of multi-filament NbTi strands in Rutherford cable, insulated with Kapton film. As such, the coil size and mechanical properties are critical in achieving the desired prestress and field quality targets for the agent. Throughout the model magnet program, different design and manufacturing techniques have been studied to obtain coils with the required mechanical properties. This paper summarizes the structural material and coil mechanical properties, coil design optimization results and production experience accumulated in the model R&D program.

I. INTRODUCTION

When manufacturing coils for superconducting magnets, mechanical properties need to be controlled within specifically defined limits. This is necessary to optimize prestress and magnetic field quality. In the LHC IR Quadrupole program at Fermilab [1], manufacturing techniques have been used to adjust azimuthal size, modulus of elasticity (MOE), and “springback”, or longitudinal shrinkage of the coils. Coil azimuthal size and MOE are controlled during manufacturing by adjusting the mold cavity size and the amount of Kapton® insulation applied to the cable. Springback is controlled by strand or cable annealing process, curing temperature and curing pressure.

A total of approximately 120 coils have been fabricated, of two different types (inner and outer layer). Inner cable has 37 or 38 strands, each 0.808 mm in diameter. Outer cable has 46 strands, each 0.648 mm in diameter. The nominal inner cable insulation system consists of 25 μm thick Kapton with 50% overlap surrounded by 50 μm Kapton with 2mm gaps. The outer cable system consists of 25μm Kapton with 50% overlap surrounded by 25μm Kapton with 50% overlap. All Kapton is 9.5mm wide. For both inner and outer coils, the outside surface of the outer layer is coated with adhesive.

Many factors affect coil azimuthal size and MOE, including bare cable size, mold cavity size, cable insulation thickness, type of insulation adhesive, strand coating and degree of strand anneal. This study focuses on the two parameters that can be controlled during the coil manufacturing process, curing cavity size and cable insulation thickness [2]. Coil size is defined as the azimuthal

length of one octant of the magnet “with respect to nominal”, that is, with respect to the coil size in an undeflected cross section. Coils are measured at room temperature at an azimuthal pressure of 80MPa. Coil MOE is the azimuthal Young’s Modulus measured between 65 and 95 MPa. Table 1 consists of features from samples used in Figures 1-10. Inner and outer coils have 14 and 16 turns, respectively, each with one insulated wedge. All samples have uncoated, unannealed strand. Sample size ranges from 5 to 22 coils.

TABLE 1
SUMMARY OF FEATURES FROM SAMPLES USED IN FIGURES 1-10

Figure, Sample No.	Ins. Thick-ness (μm)	Total Ins. in sample (μm)	Cavity Size (μm)	Cable Midthi ckness (mm)	Str- and No.	Ad- hesive
F1&3,S1	97.1	2913	varies	1.457	38	poly
F1&3,S2	98.7	2961	varies	1.457	38	poly
F1&3,S3	98.7	2961	varies	1.457	38	epoxy
F1&3,S4	98.7	2961	varies	1.465	38	poly
F2&4,S1	97.7	3321	varies	1.146	46	epoxy
F2&4,S2	97.7	3321	varies	1.146	46	poly
F6&8,S1	varies	varies	500	1.457	38	poly
F6&8,S2	varies	varies	50	1.465	37	poly
F7&9,S1	varies	varies	125	1.146	46	epoxy
F7&9,S2	varies	varies	125	1.146	46	poly

II. EFFECTS OF ADJUSTING CAVITY SIZE

Figure 1 shows size data for several samples of inner coils. Within each sample, all parameters except cavity size (cable size, strand anneal, strand number and insulation thickness) are identical. The parameters may vary between samples. Each point on the plot represents an average of several coils.

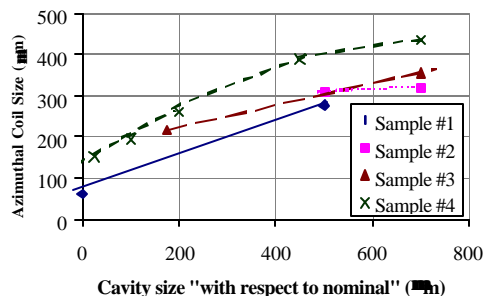


Fig. 1. Inner coil size vs. Curing Cavity Size

As expected, coil size increases with increasing cavity size. Also, the ratio between change in cavity size and coil size increases as the cavity size gets larger. Outer coils show a similar pattern, as shown in Figure 2.

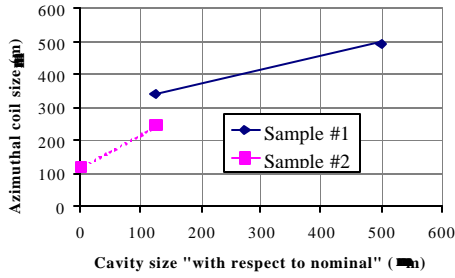


Fig. 2. Outer coil size vs. Curing Cavity Size

There is also a direct relationship between curing cavity size and azimuthal MOE. Figures 3 and 4 show the relationship between cavity size and MOE among the same samples of inner and outer coils, respectively.

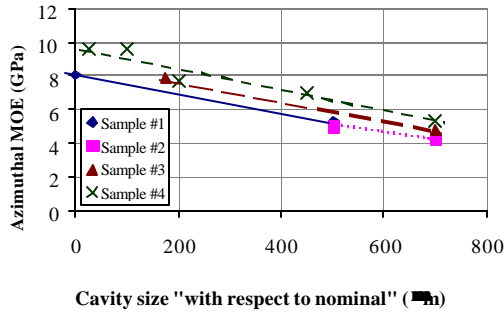


Fig. 3. Inner coil MOE vs. Curing Cavity Size

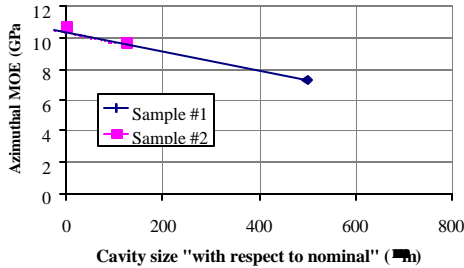


Fig. 4. Outer coil MOE vs. Curing Cavity Size

MOE decreases with increasing cavity size. This is the direct result of decreasing curing pressure. The ratio of MOE change to cavity size change does not increase significantly with increasing curing pressure over the range measured, although inner coil sample #2, which has a very low MOE range of 4.3 to 5 GPa, is slightly less sensitive to cavity size adjustment.

It is clear from Figures 1 and 2 that the cavity size-to-coil size ratio becomes larger as cavity size increases (and consequently as applied curing pressure decreases). This is shown in Figure 5 by plotting the cavity size-to-coil size ratio (the slopes in Figures 1 and 2) with respect to curing pressure, since the azimuthal pressure on the coil is prohibitively difficult to measure directly during the curing process. This is true because some of the

azimuthal hydraulic pressure applied during curing is absorbed by the mold cavity. Azimuthal coil MOE is closely correlated with curing pressure [3], and can be measured precisely for each coil.

The ratio is approximately 1:1 at high curing pressures and approaches infinity as curing pressure decreases to zero. This occurs around 4 GPa for inner coils, but may be higher for outers. So as coils get stiffer, they become more sensitive to cavity size changes.

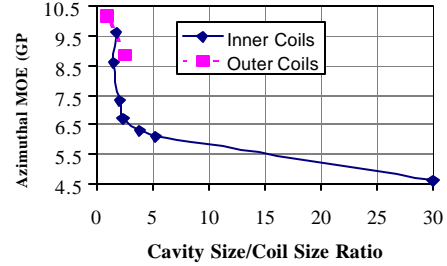


Fig. 5. Cavity size/Coil size ratio vs. Azimuthal MOE. Each point on this graph represents the slope of a line in Figures 1 or 2 vs. the average MOE for the set of coils that comprises that line. Sample 4 in Figures 1 and 3 has a point representing each component of the line.

III. EFFECTS OF ADJUSTING CABLE INSULATION THICKNESS

Another way of adjusting coil size is to vary the amount of Kapton insulation wrapped around the cable by increasing or decreasing the overlap percentage. “Integrated amount of cable insulation” is defined as the average thickness of insulation on the surface of the cable, similar to a “packing factor”. Total insulation thickness is the sum of the insulation wrapped on each cable in the azimuthal direction of the coil. Figures 6 and 7 show the relationship between total cable insulation thickness and coil size. Within each sample, all other manufacturing parameters, such as cable size and cavity size, are identical.

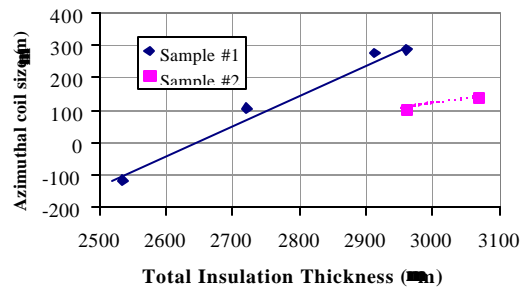


Fig. 6. Inner Coil Size vs. Cable Insulation Thickness

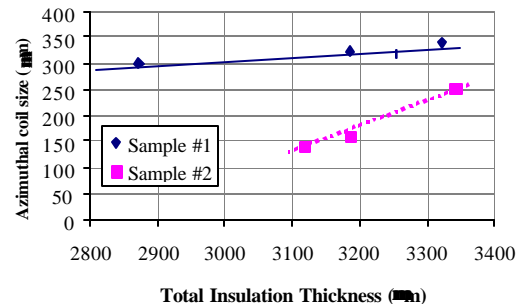


Fig. 7. Outer Coil Size vs. Cable Insulation Thickness

The effect of increasing cable insulation thickness on MOE is shown in Figures 8 and 9, using the same samples as Figures 6 and 7. Inner MOE increases by about 1 GPa per 400 μm of added insulation. This is smaller than the effect of cavity size changes on MOE, where cavity size changes of 400 μm cause MOE changes of about 2 GPa. The MOE increase may be due to an “effective” cavity size decrease from increasing the insulation thickness while keeping the actual cavity size constant. This effect is somewhat smaller than the direct effect of cavity size changes, because of the compression of the added kapton under pressure and temperature.

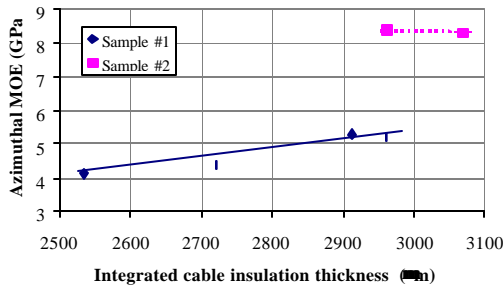


Fig. 8. Inner Coil MOE vs. Cable Insulation Thickness

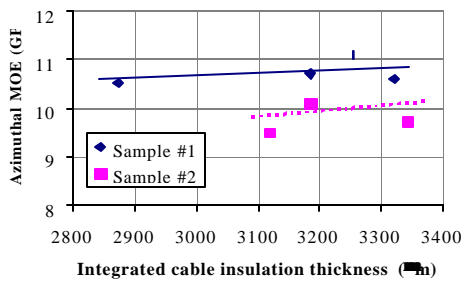


Fig. 9. Outer coil MOE vs. Cable Insulation Thickness

By comparing Figures 6 and 7 with Figures 8 and 9, it can be seen that the ratio of change in cable insulation thickness to coil size increases with the stiffness of the coil. So, within the range observed, as coils get stiffer, they become less sensitive to cable insulation thickness adjustments. This is shown in Figure 10 by plotting the cable insulation-to-coil size ratio (the slopes in Figures 6 and 7) with respect to MOE (the average values of each sample in Figures 8 and 9).

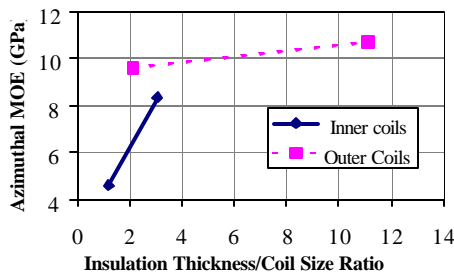


Fig. 10. Insulation Thickness/Coil Size Ratio vs. Azimuthal MOE. Each point in Figure 10 represents the slope of a line in Figure 6 or 7 vs. the average MOE for the set of coils which comprises that line.

IV. APPLICATION OF SIZE AND MOE ADJUSTMENTS

Coil size and MOE targets evolved during the production of the LHC IR Quadrupoles, and were finally set at 250 μm and 10 GPa for both inner and outer coils to achieve the

prestress goal of 75Mpa. Relationships derived from the above data were used to control coil size and MOE. R&D coils were wound, cured and measured. First, cavity size was adjusted until the target MOE was reached. Then, insulation thickness was altered to achieve the appropriate coil size. Figures 11 and 12 show the progression of coil size and MOE for the eight magnets produced in the LHCIR model coil program. When the coils are assembled into a magnet, they are arranged to minimize the differences in size between quadrants, and consequently the preload variations within the magnet. Using this process, mean coil size differences between quadrants are typically reduced to around 10 μm .

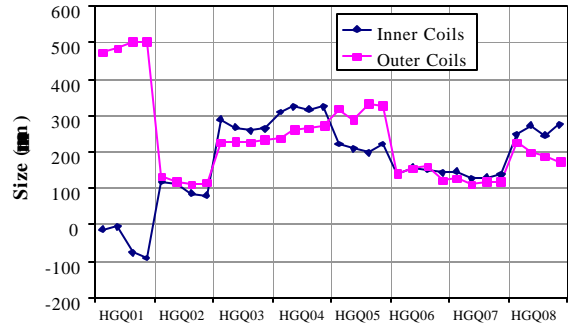


Fig. 11. Coil size in LHCIR Quadrupoles

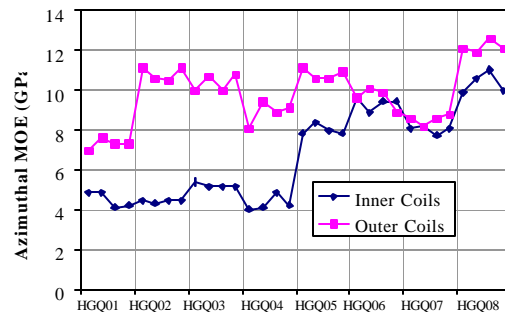


Fig. 12. Coil MOE in LHC IR Quadrupoles.

The above data represents coil mean sizes. Peak to peak variations in size over the coil straight section are typically less than 35 μm for both inner and outer coils, with a typical standard deviation of about 12 μm . MOE peak to peak variations are less than 1 GPa with typical standard deviations of about 0.4GPa.

V. SPRINGBACK

LHC IR coils are wound and cured using steel tooling which fixes the coil to a specific length of 1.5 meters. When the coil is removed from the tooling after curing, the coil shrinks longitudinally, relieving the stress incurred during the winding and curing process. The cause of this internal stress is not well understood, but it can vary depending on many factors, including curing pressure, curing temperature, and strand annealing process. Coil longitudinal shrinkage, or “springback”, is defined as the difference in length in the straight section (excluding the ends) between the length

defined by the curing tooling and the coil in the relaxed state. The length measured is shown in Figure 13.

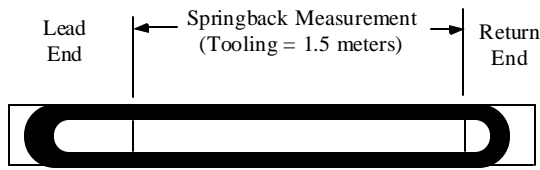


Figure 13. Springback Measurement Position

Figures 14 and 15 show the springback for a series of inner and outer LHCIR Quadrupole coils, respectively [4]. Each point represents one coil. Springback is plotted vs. coil azimuthal MOE. There are two sets of inner coils measured, one with unannealed strands, and one with strands annealed before the cable was manufactured. Both sets of coils were cured using polyimide adhesive at 190 degrees C. All were wound with the same tension of 320N. The coils with unannealed strand have more springback than those with annealed strand. In each case, springback increases with increased MOE, implying that increased azimuthal curing pressure increases springback.

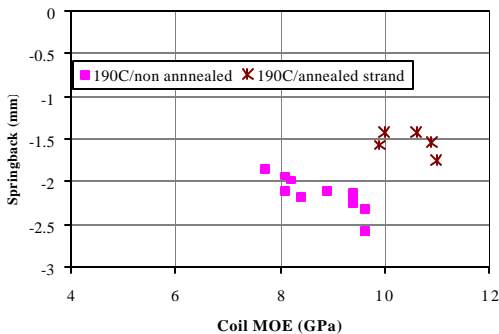


Figure 14 Springback in LHC IR Quadrupole Inner Coils

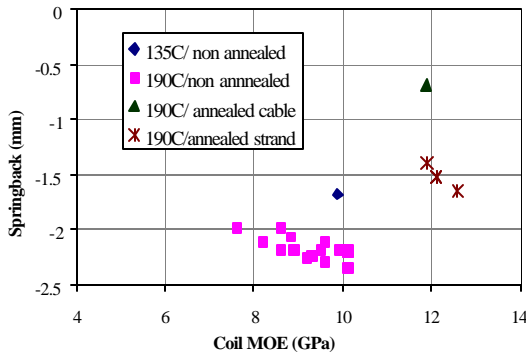


Figure 15 Springback in LHC IR Quadrupole Outer Coils

Outer coils show the same pattern. In this case, there is also a coil cured with epoxy adhesive at 135C with unannealed strand. Although there is only one coil shown, it has less springback than coils with similar MOE cured at 190C. There is also one outer coil cured with cable which was preheated to 190C for 1/2 hour after cable manufacturing, but before winding. It has the least springback, indicating that some of the internal stresses that are relieved during the

curing process are created during the cable manufacturing process. Most of the LHC IR Quads have unannealed strand and are cured at 190C. No performance problems have been attributed to the springback from these coils.

An attempt to measure coil longitudinal properties was made using cable stacks. Several stacks, each consisting of four pieces of LHC IR Quad cable, flipped alternately so that they formed a rectangular cross section, were cured with curing pressures of zero, 25MPa and 83MPa [5]. Both the azimuthal and longitudinal modulus of elasticity of the stacks were measured. Stacks cured with a higher azimuthal pressure had a higher azimuthal MOE, but as shown in Figure 16, a lower longitudinal MOE than the stacks cured with lower curing pressure. Thus, coils with higher azimuthal moduli have lower longitudinal moduli, which may in turn yield higher springback. This data supports the relationship between springback and azimuthal MOE shown in Figures 14 and 15.

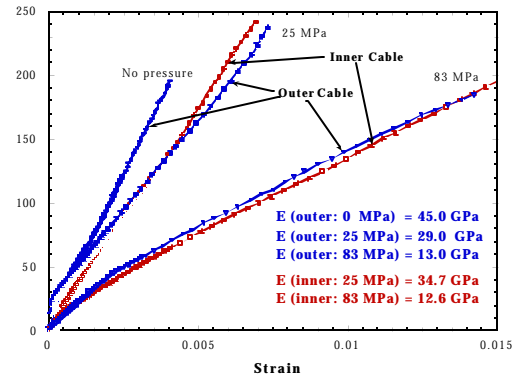


Fig. 16 Longitudinal MOE of LHCIR Quadrupole Stacks cured with Different Curing Pressures.

VI. SUMMARY

Coil azimuthal size and modulus of elasticity affect magnet performance by determining prestress, which in turn affects magnet performance. Springback may be an important factor in understanding coil longitudinal motion. These properties have been measured and controlled in LHCIR Quadrupoles by utilizing the methods described above.

ACKNOWLEDGMENTS

The authors would like to acknowledge the support of Technical Division personnel at Fermilab.

REFERENCES

- [1] N. Andreev et al., "Recent Results from the LHC Inner Triplet Quadrupole Development Program at Fermilab", *MT16 Proceedings*, 1999, in press.
- [2] R. Bossert, "HGQ Coil Manufacturing Comparisons" *Fermilab Technical Division Technical Memo*, TD-99-024.
- [3] R. Bossert, "Correlating LHC IR Quadrupole Coil MOE with Curing Pressure", *Fermilab Technical Division Technical Memo*, TD-99-043.
- [4] R. Bossert, "LHC IR Quadrupole Coil Springback Summary", *Fermilab Technical Division Technical Memo*, TD-99-044.
- [5] D.R. Chichili, et al., "Axial Mechanics of HGQ Model Magnets", *Fermilab Technical Division Technical Memo*, TD-98-061.